Superalloys 2008
Roger C. Reed, Kenneth A. Green, Pierre Caron, Timothy P. Gabb, Michael G. Fahrmann, Eric S. Huron and Shiela A. Woodard
TMS (The Minerals, Metals & Materials Society), 2008

Effect of Microstructure on Time Dependent Fatigue Crack Growth Behavior In a P/M Turbine Disk Alloy

J. Telesman[1], T.P. Gabb[1], A. Garg[2], P. Bonacuse[3] and J.Gayda[1]

[1] NASA Glenn, 21000 Brookpark Rd., Cleveland, OH 44135
[2] NASA Glenn/University of Toledo, 21000 Brookpark Rd., Cleveland, OH 44135
[3] U.S. Army Research Laboratory, Cleveland, OH 44135

Keywords: Hold time crack growth, microstructure, P/M superalloys, stress relaxation, precipitate size distribution

Abstract

A study was conducted to determine the processes which govern hold time crack growth behavior in the LSHR disk P/M superalloy. Nineteen different heat treatments of this alloy were evaluated by systematically controlling the cooling rate from the supersolvus solutioning step and applying various single and double step aging treatments. The resulting hold time crack growth rates varied by more than two orders of magnitude. It was shown that the associated stress relaxation behavior for these heat treatments was closely correlated with the crack growth behavior. As stress relaxation increased, the hold time crack growth resistance was also increased.

The size of the tertiary γ' in the general microstructure was found to be the key microstructural variable controlling both the hold time crack growth behavior and stress relaxation. No relationship between the presence of grain boundary $M_{23}C_6$ carbides and hold time crack growth was identified which further brings into question the importance of the grain boundary phases in determining hold time crack growth behavior.

The linear elastic fracture mechanics parameter, Kmax, is unable to account for visco-plastic redistribution of the crack tip stress field during hold times and thus is inadequate for correlating time dependent crack growth data. A novel methodology was developed which captures the intrinsic crack driving force and was able to collapse hold time crack growth data onto a single curve.

Introduction

The hold time fatigue crack growth behavior of nickel based powder metallurgy (P/M) turbine disk superalloys has become of paramount importance as the temperature of turbine components is increased in modern gas turbine engines. For most of the disk alloys, at temperatures 650°C or higher, the prolonged hold times at maximum stress cause the time dependent crack growth contribution to become the predominant mechanism of crack advancement by dwarfing the cyclic crack growth contribution (1).

Considerable amount of research has been performed over the years in an attempt to understand and model the hold time crack growth behavior in superalloys. One of the noted differences between hold time crack growth behavior and cyclic crack growth is the much larger variability in time dependent crack growth resistance for hold time tests. It has been shown that hold time crack growth can vary up to two orders of magnitude for the same alloy as a function of the alloy's processing history and heat treatment (1).

Researchers have shown that the typically observed intergranular failure mode for hold time crack growth is mostly the result of a preferential grain boundary attack by the environment (i.e. oxidation) at the crack tip. Based on these findings, the majority of the research has focused on grain boundary morphology in an attempt to explain and model the large variability in hold time crack growth behavior. The general assumption has been that the variability in time dependent crack growth response is due to the differences in the resistance of various grain boundary phases to environmental exposure.

Numerous grain boundary species such as carbides, borides, NiAl phases and even grain boundary misorientation have been proposed (2,3,4,5) as the species which control grain boundary environmental attack. The rationale has been the identification and replacement of grain boundary phases prone to environmental attack leading to an improvement in hold time crack growth resistance. Unfortunately none of the candidates proposed to date have withstood the test of time. Other researchers, noting that the presence of serrated grain boundaries is often associated with an improvement in hold time crack growth resistance (6), have suggested that grain boundary topographical (or mechanical) barriers to crack advancement can play an important role in determining time dependent crack growth behavior.

In both of these approaches the emphasis has been placed on the intrinsic ability of the alloy and its grain boundary structure to resist crack propagation by making the grain boundaries inert to environment or by making the crack path more tortuous. The weakness of this approach is that the entire emphasis is placed on the intrinsic ability of the disk alloys to protect the grain boundaries from attack. What is being largely ignored is the possibility that the prolonged hold times themselves can have impact on the crack tip driving forces. The crack growth data is typically correlated in terms of a linear elastic fracture mechanics stress intensity parameter, Kmax, and the comparisons drawn by comparing the hold time crack growth rates at a specified Kmax. However, the Kmax parameter does not capture any possible redistribution of the crack tip stress field which may occur during hold times.

In contrast to the prevalent hypotheses emphasizing the importance of the nature of the grain boundaries, our earlier work (7), performed on a P/M Alloy 10, showed that neither the grain boundary species previously suspected to influence grain boundary environmental resistance or the roughness of the grain boundaries were the primary variables controlling hold time crack growth resistance in this alloy. Instead, it was shown that an excellent correlation existed between the hold time crack growth

behavior and the size and volume fraction of the γ' precipitates present in the general microstructure, not at the grain boundaries. It was suggested that the strong relationship between the strengthening γ' precipitates and the hold time crack growth resistance is due to the role which the precipitate size plays in controlling the rate of stress relaxation at the crack tip during the prolong hold times at elevated temperatures. It is thus the ability of the microstructure to change the intrinsic crack driving force by a crack tip stress relaxation process which may be the critical factor influencing hold time crack growth resistance and not the morphology of the grain boundaries.

The current study examines these issues more closely by evaluating the hold time crack growth behavior of a recently developed P/M disk alloy named LSHR. The study consisted of an evaluation of the effect of microstructural parameters on hold time crack growth behavior of this alloy by systematically varying the heat treatments in order to produce a wide distribution of γ' precipitate morphology. The systematic variation of the precipitate size distribution was performed to enable a thorough investigation of the role that stress relaxation behavior may play in controlling hold time crack growth response in these types of alloys.

Nineteen different supersolvus heat treatments of this alloy were evaluated by varying the cooling rate and the aging heat treatment steps. The grain size was intentionally kept relatively constant for all microstructures in order to concentrate the research on the effect of precipitate morphology and grain boundary character.

Material and Procedure

All the specimens were blanked and machined from the same LSHR forging having composition in weight percent of 3.5Al, 0.03 B, 0.03C, 20.7Co, 12.5Cr, 2.7Mo, 1.5Nb, 1.6Ta, 3.5Ti, 4.3W, 0.05Zr, bal Ni. Each blank was individually heat treated to assure that the desired processing was achieved. Each blank was given the same supersolvus solutioning heat treatment at 1171°C. The blanks were then cooled from the solutioning temperature at either 72°C/min or 202°C/min cooling rate as measured by an embedded thermocouple. Subsequently the blanks were given either one or two step ages at various temperatures and times. The detailed list of the heat treatments is shown in Table I.

Table I. The cooling rates and the aging heat treatments investigated.

Aging Treatment	Cooling Rate-72°C/min	Cooling Rate-202°C/min
None	√	√
775°C/1 Hr	√	–
775°C/8 Hrs	√	√
815°C/1Hr	–	√
815°C/3Hr	–	√
815°C/8 Hrs	√	√
855°C/1 Hr	√	√
855°C/8 Hrs	√	√
855°C/1 Hr +775°C/8 Hrs	√	√
855°C/4 Hrs +775°C/8 Hrs	√	√
855°C/8 Hrs +775°C/8 Hrs	√	√

The blanks were used to machine both Kb bar surface flaw geometry crack growth specimens and cylindrical stress relaxation specimens. All hold time testing was conducted at 704°C with a 90 second dwell at the peak load and an R-ratio of 0.05. The crack growth measurements were obtained throughout the tests using electrical potential drop system. In addition to the hold time crack growth tests, conventional cyclic crack growth tests were conducted for selected microstructures at 427°C, at a frequency of of 0.333 Hz and R-ratio of 0.05 in order to compare the effect of microstructure on cyclic and hold time crack growth behavior.

Stress relaxation testing was conducted for all heat treatments investigated using 6.35 mm diameter cylindrical specimens machined from the heat treated blanks. The specimens were heated to 704°C and strained to 1% total strain. Stress relaxation was measured as a function of time for the 100 hour duration of the tests.

TEM and SEM

High resolution scanning electron microscopy (SEM) and transmission electron microscopy (TEM) were performed for most of the heat treatments in order to quantify the precipitate size distributions of the secondary (also know as cooling) and tertiary (also known as aging) γ' precipitate structure. For size measurement, dark-field γ' images were obtained from <100> grains oriented close to the foil normal to minimize truncation effects. Quantitative image analysis was performed on multiple images obtained from each heat treatment to measure the precipitate size distribution and volume fraction. The image analysis was performed using Sigma Scan commercial software. The grain boundary precipitates were excluded from the analysis due to insufficient number of these types of precipitates imaged during the TEM study. Thus only the intragranular precipitate populations will be discussed in the paper.

Results

Since grain size can be an important variable influencing hold time crack growth behavior, it was important to keep this variable constant in order to study the effect of other microstructural variables on crack growth resistance. By performing an identical supersolvus solutioning heat treatment on all the specimen blanks, the grain size was kept relatively constant. The mean grain size was measured for all the heat treatments studied and shown to be fairly uniform varying from an ASTM 6.6 to ASTM 7.1.

Quantitative Analysis of the γ' Precipitate Sizes

The quantitative image analysis of the precipitate size distribution obtained from TEM has been completed to date on 15 out the 19 heat treatments and the results are shown Fig. 1 and Fig. 2 in terms of the median measured precipitate size for each heat treatment investigated. Table II shows the measured area fractions of the precipitates.

Table II. Measured area fractions of the γ' precipitates.

Aging Treatment	Cooling Rate- 72°C/min		Cooling Rate- 202°C/min	
	Tertiary γ', Area Fract.	Sec. γ', Area Fract.	Tertiary γ', Area Fraction	Second. γ', Area Fraction
None	0.5	0.08	0.54	0.04
775°C/8 Hrs	0.52	0.06	0.55	0.03
815°C/3Hr			0.57	0.01
815°C/8 Hrs	0.57	0.01	0.57	0.01
855°C/1 Hr	0.53	0.05	0.54	0.04
855°C/8 Hrs	0.57	.01	0.579	0.001
855°C/1 Hr +775°C/8 Hrs	0.54	.04	0.56	0.02
855°C/4 Hrs +775°C/8 Hrs	0.51	0.07	0.55	0.03
855°C/8Hrs +775°C/8 Hrs	0.54	0.01	0.56	0.001

It was determined that the main heat treatment variable influencing the size of the secondary γ' precipitates is the cooling rate from the supersolvus solutioning step. A shown in Fig. 1, the slower cooling rate of 72°C/min resulted in larger median precipitate size than the faster cooling rate. The secondary γ' precipitates for the slow cooled treatments were 50% to 100% larger than those measured for the fast cooled treatments. The variety of subsequent aging treatments did not have a strong effect on the measured size of the secondary γ' precipitates.

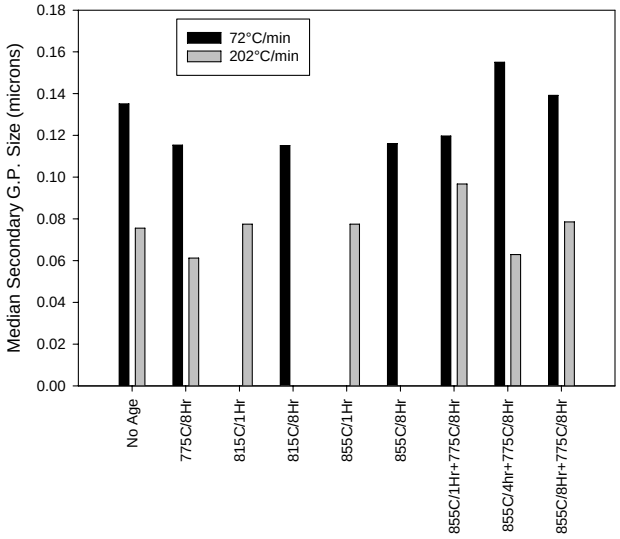

Figure 1. Median secondary γ' size measured for various heat treatments as a function of the cooling rate.

In contrast to the secondary γ' precipitates, the quantitative image analysis of the tertiary γ' precipitates revealed a strong dependence of the precipitate size on the aging heat treatments (Fig 2). The single step ages even at temperatures as low as 775°C had a pronounced effect on the size of the tertiary precipitates. The 815°C/8 hr treatment doubled the size of the precipitates while the 855°C/8 hr exposure increased over three-fold the size of the precipitates in comparison to the unaged specimen subjected to the same cooling rates. For the double step aging heat treatments, the time of exposure at the higher temperature appeared to be the critical step having the largest influence on the size of the tertiary γ' precipitates.

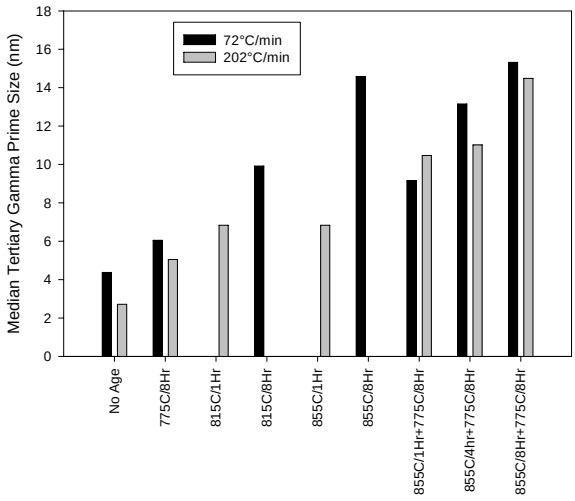

Figure 2. Median tertiary γ' size for various heat treatments investigated as a function of the cooling rate.

Grain Boundary $M_{23}C_6$ Carbides

Assessment of the grain boundary $M_{23}C_6$ carbide distribution was performed using SEM. The assessment was done on three specifically selected heat treatments chosen to represent the major heat treat variables. The $M_{23}C_6$ carbide area fraction was calculated by subtracting the MC carbide and boride area fraction from the total content and is shown in Table III. Unfortunately due to heavy concentration of the $M_{23}C_6$ carbides at the grain boundaries, it was not possible to adequately resolve the individual carbides to obtain their size distribution.

Table III. Area fractions of the $M_{23}C_6$ grain boundary carbides

Cooling Rate	Aging Treatment	Area Fraction of Grain Boundary $M_{23}C_6$ Carbides	da/dt @25MPa√m m/sec
202°C/min	775°C/8Hrs	Mean: 0.011	$1.9*10^{-7}$
		Median: 0.01	
		Std. Dev.: 0.004	
202°C/min	855°C/4 Hr +775°C/8 Hr	Mean: 0.0054	$4.3*10^{-8}$
		Median: 0.0055	
		Std. Dev.: 0.0008	
72°C/min	855°C/4 Hr + 775°C/8 Hr	Mean: 0.0049	$5.2*10^{-9}$
		Median: 0.0044	
		Std. Dev.: 0.0016	

The effect of the cooling rate on grain boundary carbide population was investigated by comparing the slow and fast cooled specimens given the identical two step aging treatment (855°C/4Hr + 775°C/8 hr). No significant differences were observed for these two cases. As shown in Table III, the mean area fraction of carbides was approximately 0.5% for both heat treatments. The carbides were distributed fairly uniformly along the grain boundaries.

The effect of the aging treatment on grain boundary carbides was investigated by comparing two fast cooled specimens, one given a 775°C/8Hr treatment while the other was subjected to previously

mentioned 855°C/4hr+775°C/8hr two step aging. Surprisingly, the specimen subjected to the lower temperature, single step aging had a larger content of grain boundary $M_{23}C_6$ carbides (~1%) than the two step heat treatment (~0.5%). Also, even though the measured area fraction for the single step age was higher, the carbides, tended to redistribute themselves more unevenly causing clumping at some grain boundaries while others were essentially carbide free. As previously mentioned, the two step aging resulted in a more uniform distribution of grain boundary carbides.

Crack Growth Results

The results of the hold time crack growth testing conducted at 704°C with a 90 second hold time period reveal that the different heat treatments evaluated resulted in a dramatic variability in the hold time crack growth resistance as shown in Fig 3. The measured hold time crack growth rates varied by more than two orders of magnitude even though the measured grain size was nearly uniform ranging from ASTM 6.6 to ASTM 7.1. In order to more closely evaluate the trends in hold time crack growth data, the measured crack growth rates at a given stress intensity Kmax of 25 MPa√m were plotted for each heat treatment and shown in Figs 4.

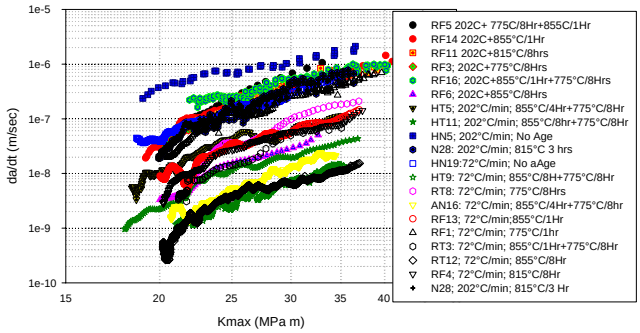

Fig 3. Hold time crack growth results for the nineteen LSHR heat treatments investigated.

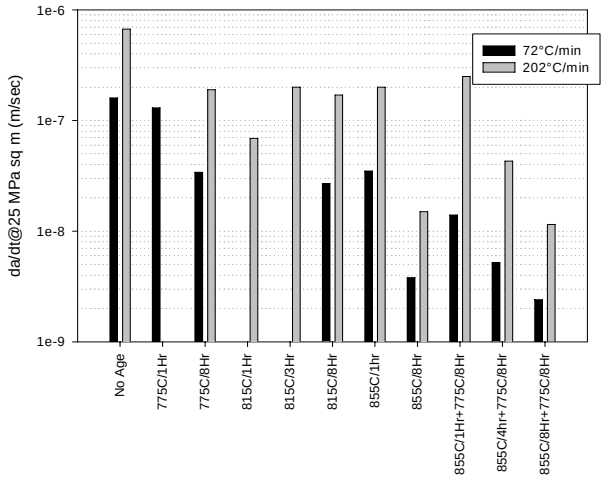

Fig 4. Hold time crack growth rates as a function of the cooling rate and aging treatment.

An examination of the results shown in Figs. 3 and 4 reveals a very consistent trend: an increase in thermal exposure results in a substantial improvement in hold time crack growth resistance. The slower cooling rate of 72°C/min resulted in a reduction in crack growth rates of 3x to 10x in comparison to the specimens cooled at 202°C/min given similar subsequent aging treatments. As shown in these figures, in addition to the cooling rate effect, the aging treatments also had a marked influence on hold time crack growth behavior. The single step aging at either 775°C/8hrs or 815°C/8 hrs produced approximately 3x to 5x improvement in hold time crack growth resistance for both cooling rates in comparison to the specimens which were not given any subsequent aging. It required only one hour at 855°C to produce the same improvement in crack growth rate as the eight hours at the lower temperatures. Increasing the aging time to 8 hours at 855°C produced approximately a further 10x improvement in crack growth resistance in comparison to the one hour exposure at the same temperature. The two stage aging treatments also resulted in substantial improvements in hold time crack growth resistance. As shown in Fig. 4, the improvement in crack growth resistance appears to be mostly governed by the exposure at 855°C with the 775°C aging treatment having a much less noticeable effect. Thus both the 855°C/1Hr+775°C/8hr and the 855°C/8hr+775°C/8hr treatments exhibited similar crack growth rates as their 855°C/1hr and 855°C/8hr single step age counterparts.

While the effect of both the cooling rate and aging heat treatment steps on hold time crack growth was dramatic, a very different behavior was observed for standard cyclic crack growth experiments performed at 427°C (typical disk bore temperatures). The cyclic crack growth tests were performed for selected heat treatments which were shown to have a large disparity in hold time crack growth behavior. The cyclic and hold time test results for three chosen heat treatments are shown in Fig. 5. While the hold time crack growth resistance differs by two orders of magnitude for these three heat treatments, the cyclic crack growth resistance for the same heat treatments tested at 427°C is essentially identical.

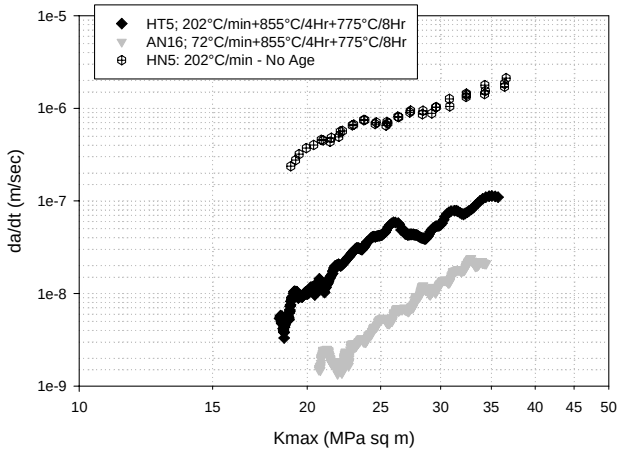

a) Hold time crack growth for three selected heat treatments at 704°C.

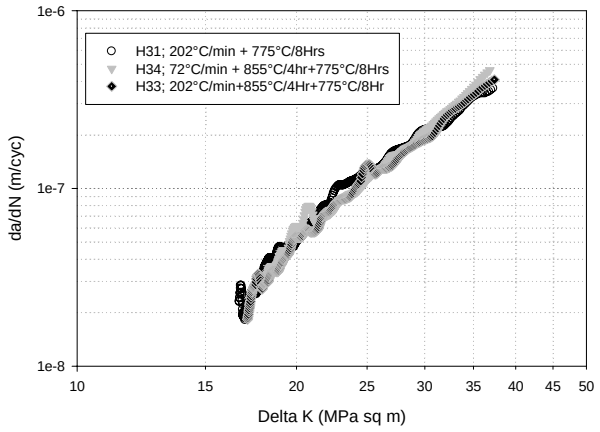

b) Cyclic crack growth behavior for the same three heat treatments at 427°C.

Fig. 5. Hold time and cyclic testing crack growth results for three selected heat treatments at 704°C and 427°C respectively.

Stress Relaxation Testing

In order to assess a possible relationship between the stress relaxation rate and hold time crack growth behavior, stress relaxation tests were performed for all the heat treat conditions. The results of the stress relaxation tests are shown in Table IV. The stress relaxation behavior was assessed by measuring the remaining stress level after 1 hour at a 1% total strain at 704°C.

Table IV. Stress Relaxation Behavior Measured at 704°C.

Aging Treatment	Cooling Rate: 72°C/min	Cooling Rate: 202°C/min
	Remaining Stress* (MPa)	Remaining Stress* (MPa)
None	882	950
775°C/1 Hr	885	–
775°C/8 Hrs	872	942
815°C/1Hr	–	948
815°C/3Hr	–	–
815°C/8 Hrs	826	900
855°C/1 Hr	829	938
855°C/8 Hrs		915
855°C/1 Hr +775°C/8 Hrs	839	927
855°C/4 Hrs +775°C/8 Hrs	809	893
855°C/8 Hrs +775°C/8 Hrs	779	864

*- Remaining stress level after 1 hour at 1% total strain.

The stress relaxation results were compared to the measured hold time crack growth rates for all the heat treat conditions. As shown in Fig 6, there is a good correlation between the measured remaining stress level after 1 hour of stress relaxation and the hold time crack growth behavior. The data was fitted separately for the 72°C/min and 202°C/min cooling rates. As shown in the figure, the lower remaining stress level (more stress relaxation) corresponded to slower crack growth rates for both cooling rates. Linear regression analyses were performed for both the 72°C/min and 202°C/min cooling rates. The heat treatments given the 72°C/min cooling rate resulted in less scatter and a higher R^2=0.86 while the measured regression fit for the 202°C/min cooling rate was determined to be r^2=0.49.

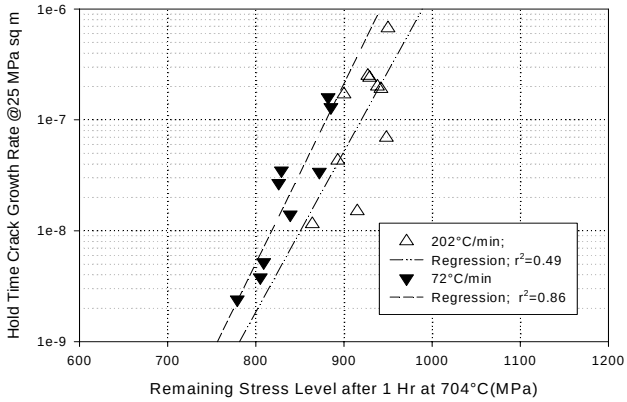

Fig 6. Relationship between the measured hold time crack growth rates and stress relaxation for both cooling rates.

The stress relaxation data was also correlated to the measured tertiary and secondary precipitate size distributions. The relationship between the tertiary precipitate sizes and stress relaxation is shown in Fig 7. As shown, there is a strong correlation for both cooling rates, with the increase in the size of the tertiary precipitates resulting in a lower remaining stress level (more stress relaxation). The 202°C/min cooling rate exhibited higher remaining stresses (less stress relaxation) than the 72°C/min cooling rate.

In contrast to the tertiary precipitates, the size of the secondary precipitates did not show a good correlation with the remaining stress level as shown in Fig 8. None the less, the smaller size of the secondary precipitates produced by the faster cooling rate was generally associated with less stress relaxation than the larger secondary precipitates produced by the slower cooling rate. However, as evident by the data scatter, the strength of that correlation was considerably weaker than for the comparable relationship for the tertiary precipitates. Thus, the tertiary γ' size distribution is a much stronger predictor of stress relaxation behavior than the secondary precipitates.

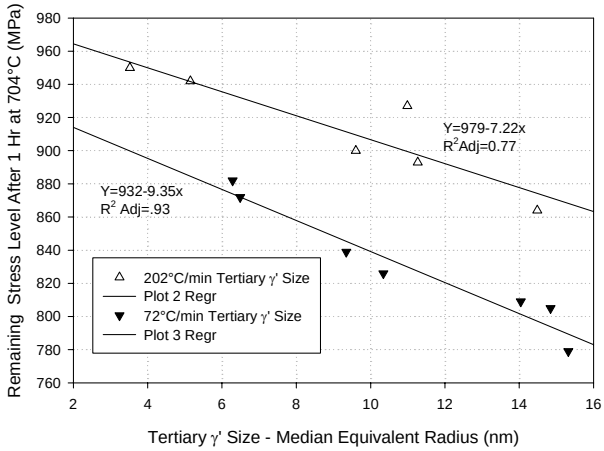

Fig. 7. A close relationship exists between the size of the tertiary γ' and stress relaxation behavior for both cooling rates.

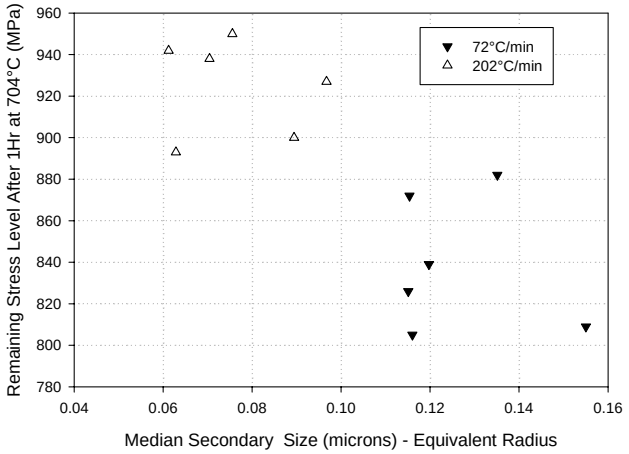

Fig. 8. The relationship between the secondary γ' and stress relaxation.

Discussion

The results of this study show conclusively that the changes in the microstructure produced by varying both the cooling rate from the supersolvus solutioning step and the subsequent aging heat treatments have a profound effect on hold time crack growth resistance at 704°C (Figs 3 and 4). As shown, the hold time crack growth resistance varied by more than two orders of magnitude as a function of thermal exposure with the slower cooling rates and longer/hotter aging steps resulting in marked improvements in the crack growth resistance.

The fractography performed on the failed specimens revealed that the hold time crack growth occurred primarily through an intergranular failure mechanism for all the different heat treatments. Our previous work (7) which focused on determining the role that the grain boundaries play in influencing hold time crack growth resistance, showed that neither the compositional variations of grain boundary carbides nor the roughness of these boundaries play a major role in determining the hold time crack growth resistance. In the current study, further effort was made to evaluate the role that the $M_{23}C_6$ grain boundary carbides play in influencing hold time crack growth behavior.

Grain boundary carbide area fraction was determined for three heat treatments which represented the extremes in hold time crack growth behavior. Both the carbide area fractions and the hold time crack growth resistance for the three selected heat treatments are detailed in Table III. As shown, the crack growth resistance for the selected heat treatments varied by two orders of magnitude. However there was no clear relationship between the $M_{23}C_6$ carbide distribution and crack growth resistance. The carbide grain boundary area fraction and distribution along the grain boundaries were virtually the same for both the fast cooled and slow cooled specimens which were given the identical 855°C/4hr + 775°C/8hr aging heat treatment. However the crack growth resistance between these two cases varied by an order of magnitude thus confirming that the grain boundary carbides are not the controlling species which determine hold time crack growth behavior.

Tertiary Precipitates and Stress Relaxation Behavior

The quantitative image analysis results of the size distribution of the secondary and tertiary precipitates suggested that the cooling rate from the solutioning step was primarily responsible for determining the size of the secondary precipitates (Fig 1) while the tertiary γ' size distribution was controlled by the aging treatments (Fig 2). The relationship between the size of the secondary and tertiary γ' precipitates and the stress relaxation behavior is shown in Figs 7 and 8. As mentioned previously, there was a strong relationship between the median size of the tertiary precipitates and stress relaxation behavior for both cooling rates. The relationship between precipitate size and stress relaxation was weaker for the secondary γ' precipitates (Fig. 8) even though their measured area fraction was approximately an order of magnitude greater than the tertiary precipitates.

The present results showing the importance of tertiary γ' precipitates on the stress relaxation behavior are in agreement with results published by Locq et. al. (8) They showed that for another P/M disk alloy, the creep behavior at 700°C is highly controlled by the presence of tertiary γ' precipitates. The particles act to impede the dislocation motion by lowering the mean free path and forcing the dislocations to cut through the precipitates. Elimination of the tertiary γ' by overaging significantly degraded creep resistance by allowing easy glide of dislocations.

The rationale employed by Locq et. al. (8) can also be used to explain the difference in the stress relaxation behavior between the two cooling rates. While the size distribution of the tertiary γ' is similar for the two cooling rates, the smaller secondary γ' precipitates found in the fast cool specimens act to strengthen the microstructure more effectively than the larger secondary precipitates produced by the slow cooling rate. This is supported by the data shown in Fig 8, where the smaller secondary precipitates found in the fast cool microstructure were generally associated with higher remaining stress levels.

Hold Time Crack Growth and Precipitate Size Distribution

In our previous work done on P/M Alloy 10 (7) we hypothesized that hold time crack growth resistance is closely linked to the stress relaxation behavior. The greater the ability of the crack tip crack driving forces to decrease through a stress relaxation mechanism during hold times, the smaller is the actual crack driving force which in turn leads to slower crack growth rates.

For the LSHR alloy, the relationship between stress relaxation behavior and hold time crack growth resistance is illustrated in Fig. 6 for both cooling rates. In general, for both cooling rates, the greater the remaining stress level (smaller stress relaxation) the higher were the hold time crack growth rates. Since stress relaxation has been shown to be mostly a function of the tertiary γ' size distribution, we can also relate the size of the tertiary precipitates to the hold time crack growth rate. As shown in Fig. 9, for both cooling rates there is a strong relationship between the median measured tertiary precipitate size and the hold time crack growth rates. As the size of the tertiary precipitates increased, the crack growth rate decreased. The linear regression curve fit, adjusted R^2 values were respectively 0.79 for the slow cooled aging treatments and 0.63 for the fast cooled treatments.

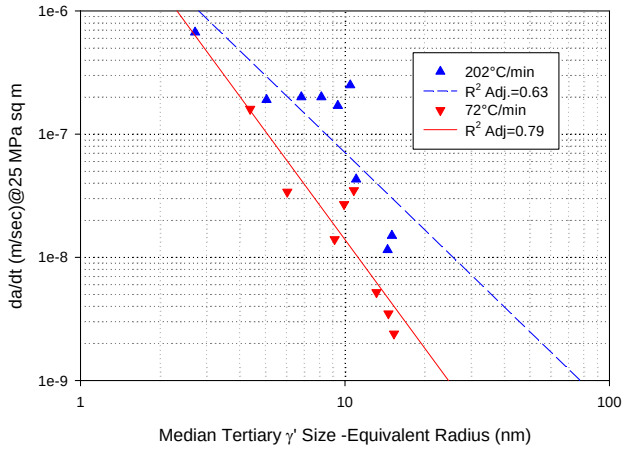

Figure 9. Relationship between tertiary precipitate size and hold time crack growth rates for the heat treatments investigated.

The relationship between the size of the secondary γ' and the hold time crack growth rates (Fig 10) is considerably weaker than for the tertiary γ'. This gives further support to the working hypothesis, since it has already been shown that the tertiary γ' precipitates have the most influence on stress relaxation behavior and thus they and not the secondary γ' precipitates should have the strongest influence on hold time crack growth behavior. The results in present study are in agreement with findings by Schirra et.al. (9). They performed a regression analysis of various microstructural parameters in two P/M alloys and found that the size of the tertiary γ' precipitates was the best predictor of hold time crack growth behavior.

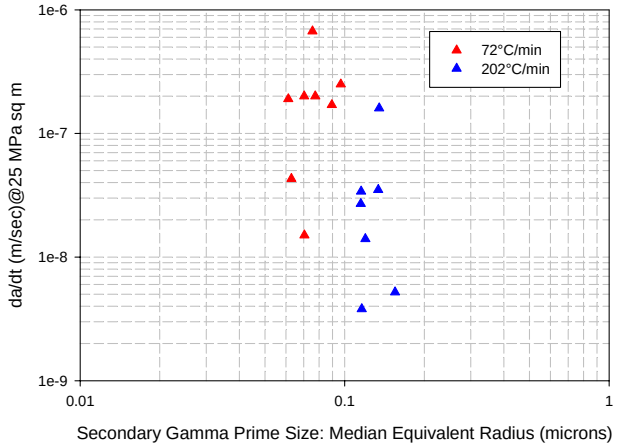

Fig 10. A weak relationship between the secondary precipitate sizes and da/dt.

Crack Tip Driving Force and Crack Growth Mechanisms

It needs to be pointed out that the there is a clear difference between the variables influencing the crack tip driving force and the mechanism of crack propagation during hold times. It is important to comprehend that even though the crack tip driving force is influenced by the stress relaxation behavior, the crack propagation mechanism still consists mainly of an environmentally assisted attack along the grain boundaries. As long as the rate of the environmental embrittlement at the crack tip is faster than the crack propagation rate, a mostly intergranular time dependent failure mechanism will predominate. Thus, while the crack driving force is a function of the stress relaxation behavior and differs substantially for the various heat treatments investigated, the crack growth mechanism for all the heat treatments is similar and governed by an intergranular environmental attack.

Probably the best illustration of the relationship between the crack driving force and environmental attack was published by Molins et. al (10). Their work was performed on IN718 tested at 650°C with 300 second hold times inside a vacuum chamber. At various stages during the hold period air was introduced for 60 seconds. If the introduction of air occurred during the early portions of the hold period, the resulting crack growth rates were similar to those obtained for baseline tests done in air. However, if the 60 second air pressure cycle was introduced during the latter stages of the 300 second hold time, the crack growth rates were a small fraction of the baseline tests performed in air. Thus the only difference between the two tests was the stage during the hold time period in which air was introduced.

These results can be explained by invoking stress relaxation behavior. When the air is introduced in the early stages of the 300 second hold cycle, the crack tip crack driving forces have not as yet relaxed significantly thus resulting in the crack growth rates comparable to the air tests. For the tests conducted with the air being introduced during the latter stages of the 300 second hold period, the crack does not advance while the hold is occurring in vacuum, however the crack tip stresses are reduced since stress relaxation can still take place. Once the air is introduced for 60 seconds the crack can begin to grow, however the rate of crack growth is much slower since the crack tip driving stresses are lower.

Our results are in an agreement with the data trends presented by Molin et.al (10). While we did not perform any testing in vacuum, we modified the microstructure in a manner which resulted in a large variability in the stress relaxation response. Thus the microstructures which produced the greatest amount of stress relaxation resulted in the slowest crack growth rates. This is analogous to the slowest crack growth rates being measured by Molin (10) when the air was introduced at the latter portions of the hold time, at which point extensive stress relaxation has already taken place resulting in slower hold time crack growth rates.

Another important finding of their work was that the damaging grain boundary process occurs very quickly over a short distance from the crack tip with nickel oxide being the first species to be embrittled. This finding was later corroborated by Browning (11). If the formation of the nickel oxide is the key to the grain boundary environmental attack, then the historical lack of success in improving hold time crack growth resistance through compositional modifications can be better understood by the difficulties encountered in attempting to suppress the formation of NiO in alloys which contain approximately 50% nickel. This argument further accentuates the need to improve the hold time crack growth resistance by focusing the effort on mechanisms which can reduce the crack driving force without extensively sacrificing other key alloy properties.

Indirect Measurements of the Crack Driving Force

In order to support the hypothesis that the crack tip driving forces are influenced by the stress relaxation behavior, an attempt was made to indirectly measure the intrinsic crack driving forces.

The amount of secondary cracking has been previously used at NASA during failure investigations to qualitatively estimate the magnitude of the stress intensity parameter. Thus, a small amount of secondary cracking is presumed to be representative of regions of low crack growth rates and relatively low stress intensities. Conversely, a high amount of secondary cracking is usually representative of high crack growth rates and higher stress intensities.

If the hypothesis is correct that the stress relaxation behavior significantly affects the crack driving forces, then it may be possible to measure the indirect manifestations of the crack tip driving forces by quantitatively examining the failure surfaces of the tested specimens. The amount secondary cracking was measured for three selected microstructures which exhibited wide variation in crack growth resistance. As shown in sample fractographs (Fig 11) the amount of observed secondary cracking did vary substantially for the three selected heat treatments, with the slow cooled specimen subjected to the two step aging treatment exhibiting the lowest amount of secondary cracking, while the fast cool specimen without aging revealed the highest amount of secondary cracking.

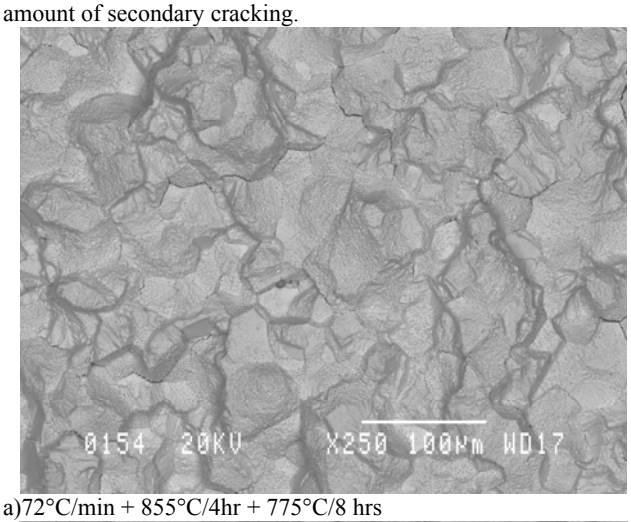

a)72°C/min + 855°C/4hr + 775°C/8 hrs

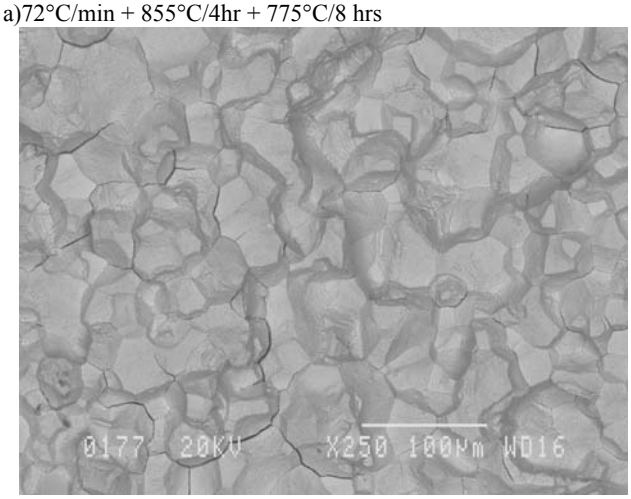

b) 202°C/min + 855°C/4hr + 775°C/8 hrs

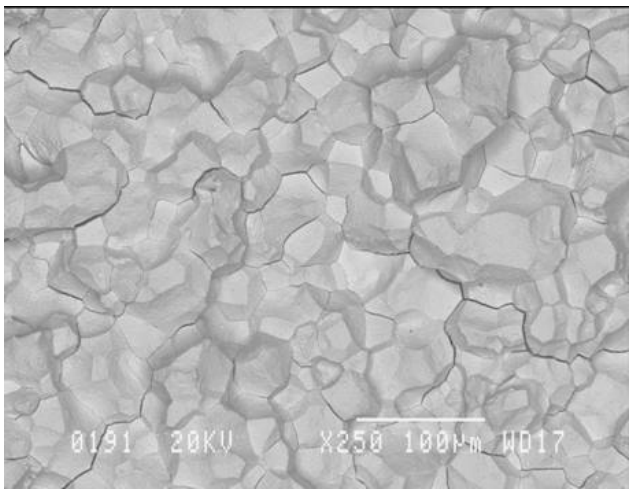

c) 202°C/min, no aging.

Fig 11. Backscatter SEM images obtained at similar stress intensities for the three heat treatments investigated.

The quantitative analysis of the amount of secondary cracking was performed by evaluating four different stress intensity regions for each specimen. At a given Kmax region, three to four backscatter images were obtained from each specimen. The images were subsequently analyzed using an automated Matlab routine written to produce a mean minus three standard deviation (-3σ) in pixel intensity thresholded image. An example of such reconstruction is shown in Fig 12. The thresholding of the images eliminated all features with the exception of the highly contrasted secondary cracks. Some additional filtering was performed to eliminate non-crack features (surface contamination, etc.) The area percent of the pixels which represented secondary cracking was then calculated by the Matlab routine.

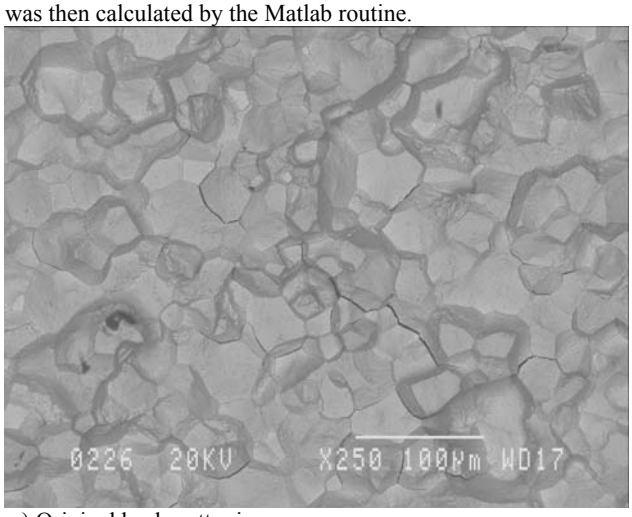

a) Original backscatter image

b) Reconstructed backscatter image after -3σ thresholding.

Fig 12. Backscatter image shown before and after thresholding was performed to isolate the secondary cracking regions.

The first test of the validity of this method was to show that the amount of secondary cracking is indeed proportional to the applied stress intensity. The percent of secondary cracking versus the calculated maximum stress intensity is plotted in Fig 13 for all three microstructures evaluated. As shown, for each microstructure the measured amount of secondary cracking does indeed increase as the stress intensity is increased. Further, as shown in the figure, at a given calculated stress intensity, there are substantial differences between the three microstructures indicating that the amount secondary cracking might be a good predictor of the crack growth rates.

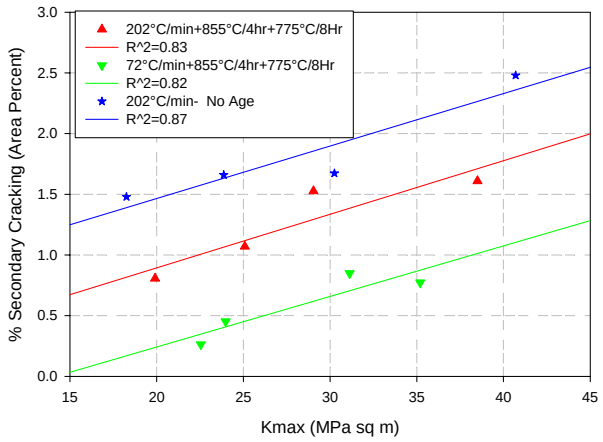

Fig 13. Secondary cracking increases for each heat treatment evaluated as a function of the applied Kmax.

Figures 14 and 15 show respectively the hold time crack growth for these selected heat treatments as correlated to the applied Kmax (Fig 14), and to the measured area percent of secondary cracking (Fig 15). In terms of the applied stress intensity, Kmax, the differences in the crack growth rates for the three heat treatments are more than two orders of magnitude. However, in terms of the percent area of secondary cracking the data collapses onto single curve.

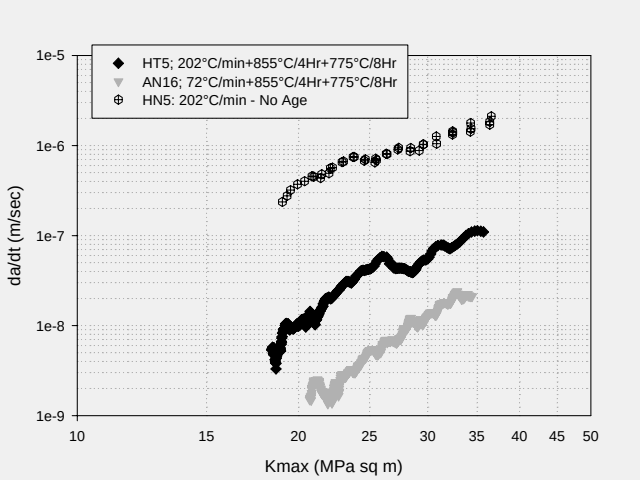

Fig 14. The hold time crack growth data plotted in terms of Kmax for the three selected heat treatments.

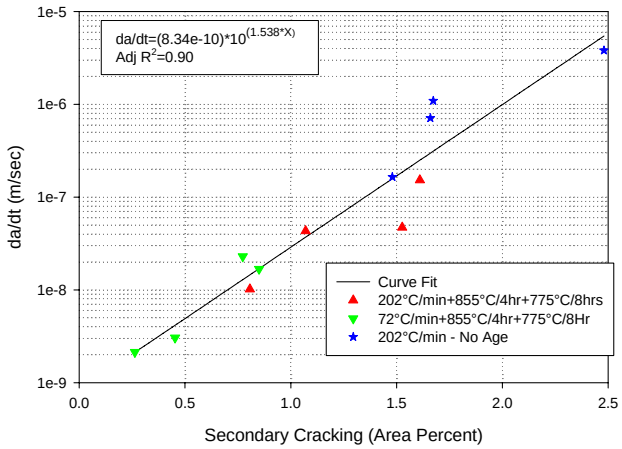

Fig 15. The crack growth data for the three heat treatments plotted in terms of the area percent of secondary cracking.

The regression analysis performed for the relationship between hold time crack growth rate and area percent of secondary cracking resulted in the following relationship:

$$da/dt = (8.34 \cdot 10^{-10})^{(1.538x)} \quad (1)$$

where da/dt is hold time crack growth rate and x is percent of secondary cracking.

The calculated adjusted R^2=0.90 shows that the above relationship does a good job in correlating the two variables. The ability of a single curve to represent the crack growth data for these three varied microstructures is a manifestation of the failure features representing the true (or intrinsic) crack tip driving forces. This should be contrasted with the inability of the Kmax parameter to collapse the same hold time crack growth data.

This analysis adds additional support to the hypothesis that the large differences in the hold time crack growth resistance measured for the various cooling rates and aging treatments are a consequence of the inability of the linear elastic fracture mechanics crack driving force parameter, Kmax, to accurately

describe the actual crack tip driving forces. This parameter does not account for the large changes in the crack tip stress relaxation behavior which were shown to occur for the different heat treatments. The area fraction of secondary cracking is a better indicator of the actual crack driving force since it is a reflection of the underlying visco-plastic redistribution of the crack tip stress and strain fields occurring during the extended hold times.

Further work is needed to validate this hypothesis by conducting a hold time crack growth study utilizing test specimen geometry and employing high resolution extensometry to enable the determination of visco-plastic fracture mechanics parameters such as C^*. The use of visco-plastic parameters to correlate the hold time crack growth data may be needed to fully describe the actual crack tip driving forces and answer some of the key remaining questions with regards to the time dependent crack growth behavior in disk alloys.

Summary

A study was conducted to determine the processes which govern hold time crack growth behavior in P/M disk superalloys. The alloy used in the study is a NASA developed LSHR P/M superalloy. While keeping the grain size relatively constant, nineteen different heat treatments of this alloy were evaluated by systematically controlling the cooling rate from the supersolvus solutioning step and by applying various single and double step aging treatments.

The study focused on the development of relationships between hold time crack growth behavior and the alloys stress relaxation properties. Furthermore, the size distribution of the γ' precipitate structure was determined since the strengthening precipitates have a strong influence on the stress relaxation behavior.

The hold time crack growth testing conducted at 704°C resulted in the crack growth resistance varying by more than two orders of magnitude for the various heat treatments. In contrast, no significant differences in cyclic crack growth resistance were noted for testing conducted at 427°C. The increase in thermal exposure generated by either slowing the cooling rate from the solutioning step and/or by exposing the specimens to hotter/longer aging steps progressively improved the hold time crack growth resistance.

Stress relaxation testing conducted on the specimens given the same series of heat treatments showed an inverse relationship in comparison to the hold time crack growth results with an increase in thermal exposure resulting in greater amount of stress relaxation. The mean size of tertiary precipitates was found to be the most important microstructural variable having the largest influence on both hold time crack growth and stress relaxation. The secondary γ' precipitates were weakly related to these properties. No relationship between the grain boundary $M_{23}C_6$ and hold time crack growth was identified which further brings into question the importance of the grain boundary phases in determining hold time crack growth behavior.

The data supports the hypothesis that the dominant mechanism which has the largest influence on the hold time crack growth behavior is the ability to reduce the crack tip stress driving forces by stress relaxation. The linear elastic fracture mechanics parameters typically used to correlate time dependent crack growth behavior do not account for the visco-plastic redistribution of the crack tip stress and strain fields occurring during the extended hold times.

While the hold time crack growth occurs mostly by an intergranular embrittlement of grain boundaries for all the heat treatments, the crack driving force changes significantly for each heat treatment based on the ability of the given microstructure to relax the crack tip driving stress. The apparent differences in the hold time crack growth response are a manifestation of the inability of the Kmax parameter to account for crack tip relaxation.

A novel method was developed to indirectly measure the true intrinsic crack driving force was able to collapse the crack growth data for various heat treatments onto a single curve. The same crack growth data plotted in terms of Kmax varied by two orders of magnitude.

References

1) K.M. Chang, M.F. Henry and M.G. Benz, "Metallurgical Control of Fatigue Crack Propagation in Superalloys" , JOM, , 42, 1990, pp. 29-35.
2) M. Gao, D.J. Dwyer and R.P. Wei, Scripta. Met. et Mater., Vol. 32, No.8, 1995, pp. 1169-1174.
3) K.R. Bain and R.M. Pelloux, Metall. Trans. A, 1984,15A.
4) L. Ma, K.M. Chang, S.K. Mannan, S.J. Patel, Scripta Materialia, Vol. 48, 2003, pp 551-557.
5) U. Krupp, W.M. Kane, X. Liu, O. Dueber, C. Laird, C.J. McMahon Jr., " The effect of grain-boundary-engineering-type processing on oxygen induced cracking of IN718", Mat. Science and Eng., A349, 2003, pp 213-217.
6) H. Loyer Danfou, M. Marty, A. Walder, "Formation of Serrated Grain Boundaries and Their Effect on the Mechanical Properties in a P/M Nickel Base Superalloy", Superalloys 1992, ed. S.D. Antolovich et.al., 1992, pp. 63-72.
7) J. Telesman, P. Kantzos, J. Gayda, P.J. Bonacuse and A. Prescenzi,"Microstructural Variables Controlling Time-Dependent Crack Growth in a P/M Superalloy" , Superalloys 2004, ed K.A. Green et.al., 2004, pp. 215-224.
8) D. Locq, P.Caron, S. Rajouf, F. Pettinari-Sturmel, A. Coujou and N. Clement, "On the Role of Tertiary γ' Precipitates in Creep Behaviour at 700°C of a PM Disk Superalloy", Superalloys 2004. pp 179-187.
9) J.J. Schirra, P. Reynolds, " Effect of Microstructure and Heat Treatment on the 649°C Properties of Advanced P/M Superalloy Disk Materials, Superalloys 2004, TMS, pp.341-350.
10) R. Molins, G. Hochstetter, E. Andrieu, Acta. Mater. Vol 45, No2, 1997, pp. 663-674.
11) P.F. Browning, "Time Dependent Crack Tip Phenomena in Gas Turbine Disk Alloys", PhD Thesis, Rensellaer Polytechnique Institute, Troy, New York, 1998.